Biochemical and Biophysical Research Communications 456 (2015) 649–655

Contents lists available at ScienceDirect

Biochemical and Biophysical Research Communications

journal homepage: www.elsevier.com/locate/ybbrc

Porcine parvovirus infection induces apoptosis in PK-15 cells through activation of p53 and mitochondria-mediated pathway

Hongling Zhang [1], Yong Huang [1], Qian Du, Xiaomao Luo, Liang Zhang, Xiaomin Zhao, Dewen Tong *

College of Veterinary Medicine, Northwest A&F University, Yangling, Shaanxi 712100, PR China

ARTICLE INFO

Article history:
Received 24 November 2014
Available online 10 December 2014

Keywords:
Porcine parvovirus
PK-15 cells
Apoptosis
The mitochondrial pathway
Caspase
p53 protein

ABSTRACT

Porcine parvovirus (PPV) infection has been reported to induce the cytopathic effects (CPE) in some special host cells and contribute the occurrence of porcine parvovirus disease, but the molecular mechanisms underlying PPV-induced CPE are not clear. In this study, we investigated the morphological and molecular changes of porcine kidney cell line (PK-15 cells) infected with PPV. The results showed that PPV infection inhibited the viability of PK-15 cells in a time and concentration dependent manner. PPV infection induced typical apoptotic features including chromatin condensation, apoptotic body formation, nuclear fragmentation, and Annexin V-binding activity. Further studies showed that Bax was increased and translocated to mitochondria, whereas Bcl-2 was decreased in PPV-infected cells, which caused mitochondrial outer-membrane permeabilization, resulting in the release of mitochondrial cytochrome c, followed by caspase-9 and caspase-3 activation. However, the expression of Fas and Fas ligand (FasL) did not appear significant changes in the process of PPV-induced apoptosis. Moreover, PPV infection activated p53 signaling, which was involved in the activation of apoptotic signaling induced by PPV infection via regulation of Bax and Bcl-2. Taken together, our results demonstrated that PPV infection induced apoptosis in PK-15 cells through activation of p53 and mitochondria-mediated apoptosis pathway. This study may contribute to shed light on the molecular pathogenesis of PPV infection.

1. Introduction

Porcine parvovirus (PPV), a member of the autonomous Parvovirus, belonging to the genus *Parvovirus* of the family *Parvoviridae*, is a major infectious pathogen of reproductive failure in swine [1]. PPV can spread primarily through vertical transmission during gestation, causing early embryonic death, fetal mummification, stillbirths, infertility and delayed return to estrus, resulting in enormous economic losses for livestock industry [2,3]. Histological lesions in kidney and other tissues of swine fetuses have been demonstrated following either natural [4] or experimental PPV infection [5,6], which characterized by cellular infiltration with little cellular necrosis indicative of a host inflammatory [7]. In line with in vivo pathologic changes, PPV also induces CPE when propagated in swine testis (ST) cells [8].

Apoptosis is a major approach in virus-induced pathophysiological changes and cytopathic effects [9]. Apoptotic cell death occurs in various virus infectious swine diseases, such as transmissible gastroenteritis virus (TGEV) [10], swine fever virus (SFV) [11] and porcine reproductive and respiratory syndrome virus (PRRSV) [12]. Parvoviruses also have been reported to trigger apoptosis in host cells. Canine parvovirus type 2a (CPV-2a) infection in MDCK cells induces apoptosis through extrinsic and intrinsic pathways [13]; bocavirus minute virus of canines (MVC) infection induces apoptosis in canine cells via mitochondrion-mediated apoptosis pathway [14]; human parvovirus B19 (B19V) infection induces apoptosis by tumor necrosis factor alpha pathways [15]. However, little is known about the molecular mechanisms of PPV-induced apoptosis.

In the present study, we investigated the effects of PPV infection in PK-15 cells. The morphological and molecular changes in PPV-infected cells suggested that PPV infection induced apoptosis through activation of p53 and mitochondria-mediated pathway.

2. Materials and methods

2.1. Antibodies, cells and virus

Monoclonal antibodies against Fas, FasL, Bid, Bax, Bcl-2, cytochrome c, poly (ADP-ribose) polymerase (PARP), β-actin, Cox4 and Histone were purchased from Santa Cruz Biotechnology (Santa

* Corresponding author. Fax: +86 29 87091032.
E-mail address: dwtong@nwsuaf.edu.cn (D. Tong).
[1] These authors contributed equally to this work.

http://dx.doi.org/10.1016/j.bbrc.2014.12.011
0006-291X/

Cruz, Inc., CA, US). Horseradish peroxidase (HRP)-conjugated secondary antibody was purchased from Pierce (Pierce, Rockford, IL, US). Porcine kidney (PK-15) cells (ATCC, CCL-33) were cultured in Dulbecco's Modified Eagle's Medium (Gibco BRL, Gaithersburg, MD, US) supplemented with 10% heat-inactivated fetal bovine serum (Thermo Scientific HyClone, Beijing, China), and incubated at 37 °C in a 5% CO_2 atmosphere incubator. The PPV YL strain was isolated from liver of PPV infected piglets in Shaanxi Province of China and identified by physicochemical test, neutralization test, RT-PCR and sequence analysis [16]. Partial DNA sequence of PPV YL has been submitted to GenBank (Accession No. JN860197.1). Virus titers were determined by 50% tissue culture infective doses ($TCID_{50}$) assay according to Reed and Muench method [17], the PPV YL strain at a titer of $10^{8.11}$ $TCID_{50}$/ml.

2.2. Cell viability assessment

The effects of PPV on PK-15 cells viability was determined by MTT assay as described previously [18]. Briefly, 1×10^4 cells per well were seeded into 96-well plates and infected with PPV at multiplicity of infection (MOI) (0.5, 1, 2, 4, 8 MOI) for different times. Meanwhile, negative controls and blank controls were set up. 3-(4, 5-Dimethylthiazol-2-yl)-2,5-diphenyltetrazolium bromide (MTT, 5 mg/ml) was added to per well and kept at 37 °C for 4 h. Then dimethyl sulfoxide (DMSO) was used to dissolve the resulting formazan crystals, the absorbance was measured by microplate spectrophotometer (Infinite 200 PRO NanoQuant, Tecan, Switzerland) at 570 nm.

2.3. Apoptosis assessment by AO/EB staining

PK15 cells in exponential growth were seeded into 24-well culture plates and infected with PPV at 1.0 MOI for different times. The cells were stained with 100 μl of fresh-prepared acridine orange/ethidium bromide staining solution (AO/EB, 100 μg/ml) and incubated at room temperature for 5 min in the dark, then observed under a fluorescence microscope (Nikon, Inc., Tokyo, Japan) in less than 20 min.

2.4. DNA fragmentation assay

Cells with different treatments were collected and washed with phosphate-buffered saline (PBS), pellets were then lysed with DNA lysis buffer (20 mM EDTA, 100 mM Tris, pH 8.0, 0.8% SDS) at room temperature for 1 h. After centrifugation for 10 min at 12,000 × *g*, the supernatant was collected and treated with RNase A (final concentration, 500 μg/ml) for 1 h at 37 °C, followed by digestion with proteinase K (final concentration, 500 μg/ml) for 2 h at 55 °C. After that, isometric phenol/chloroform/isoamylol (25:24:1) was added and centrifuged for 10 min at 12,000 × *g*, the supernatant was collected and precipitated with 3 M NaAc and ethanol for overnight. The DNA was dissolved in TE buffer (10 mM Tris, 1 mM EDTA, pH 8.0), and loaded onto 2.0% agarose gel electrophoresis for DNA fragmentation analysis.

2.5. Quantification of apoptotic cells by flow cytometry

Annexin V-FITC/PI apoptosis detection kit (Keygen Biotech, China) was used to detect the percentage of cells undergoing apoptosis according to the manufacturer's protocol. The infected and mock cells were digested by trypsinization without EDTA and washed with ice-cold PBS for 3 times. The precipitation after centrifugation was suspended with 500 μl binding buffer, followed by the addition of 5 μl Annexin V-FITC and 5 μl propidium iodide (PI), the mixture was then incubated at room temperature for 15 min in the dark. The stained cells were analyzed by flow cytometry (Beckman Coulter, Inc., Fullerton, CA, US) within an hour.

2.6. Caspase activity assay

Caspases colorimetric assay kits (Keygen Biotech, China) were used to measure the activity of caspase-3, caspase-8 and caspase-9 respectively. According to the manufacture's recommendations, the cells were treated with lysis buffer, protein concentration was measured using BCA Protein Assay Reagent (Vazyme, NJ, US). Then 200 μg lysates of each sample were loaded into microplates and incubated with each caspase substrate at 37 °C for 4 h, after that, the absorbance values of samples were measured at 405 nm in microplate spectrophotometer (Infinite 200 PRO NanoQuant, Tecan, Switzerland).

2.7. Western blot analysis

Protein extraction and western blot assay were performed as previously described [18]. The PPV-infected cells were harvested, washed with ice-cold PBS and lysed with ice-cold RIPA lysis buffer with 1 mM phenylmethyl sulfonylfluoride (PMSF) (Beyotime Inst. Biotech, Beijing, China). Mitochondrial and cytosolic proteins were isolated using the Mitochondria/cytosol Fractionation Kit (Pierce, Rockford, IL, US) according to the manufacturer instructions. Protein concentration was determined using BCA Protein Assay Reagent. Equivalent amounts of proteins were subjected to 8–12% SDS–PAGE and electrophoretically transferred to polyvinylidene difluoride (PVDF) membrane (Millipore Corp, Atlanta, GA, US). The blots were blocked in PBS buffer with 5% non-fat dry milk at room temperature for 1 h. Then, indicated primary antibodies and HRP-conjugated secondary antibodies were incubated respectively. Signals were visualized by enhanced chemiluminescence (ECL) reagent (Pierce, Rockford, IL, US).

2.8. Statistical analysis

Data were shown as means ± SEM values of three independent experiments. Each experiment was carried out in triplicate. Statistical comparison of the results was analyzed by oneway analysis of variance (ANOVA). A value of $P < 0.05$ was considered significant.

3. Results

3.1. PPV infection inhibited the growth of PK-15 cells

To assess the effect of PPV infection on the growth of PK-15 cells, we firstly investigated the viability of PPV-infected cells. At 24 h post infection (p.i.), a significant inhibition of cellular viability appeared in PK-15 cells infected with PPV more than 1.0 MOI, and became more evident with the increase of virus titers and infection time (Fig. 1A). This result demonstrated that PPV infection inhibit the growth of PK-15 cells in a time and dose dependent manner.

3.2. PPV infection induced apoptosis in PK-15 cells

To investigate whether apoptosis occurred in the process of PPV-induced cell death, we observed the morphological and molecular changes of PK-15 cells infected with 1.0 MOI of PPV for indicated times. Annexin V and PI staining assay showed that the apoptosis rate significantly increased at 12 h p.i. in PPV-infected cells when compared with mock-infected population (Fig. 1B). CPE appeared at 24 h p.i., and became evident at 36 h p.i., and 48 h p.i. (Fig. 1C, upper panel). Consistent with this change, typical apoptotic features of nuclear morphology were observed

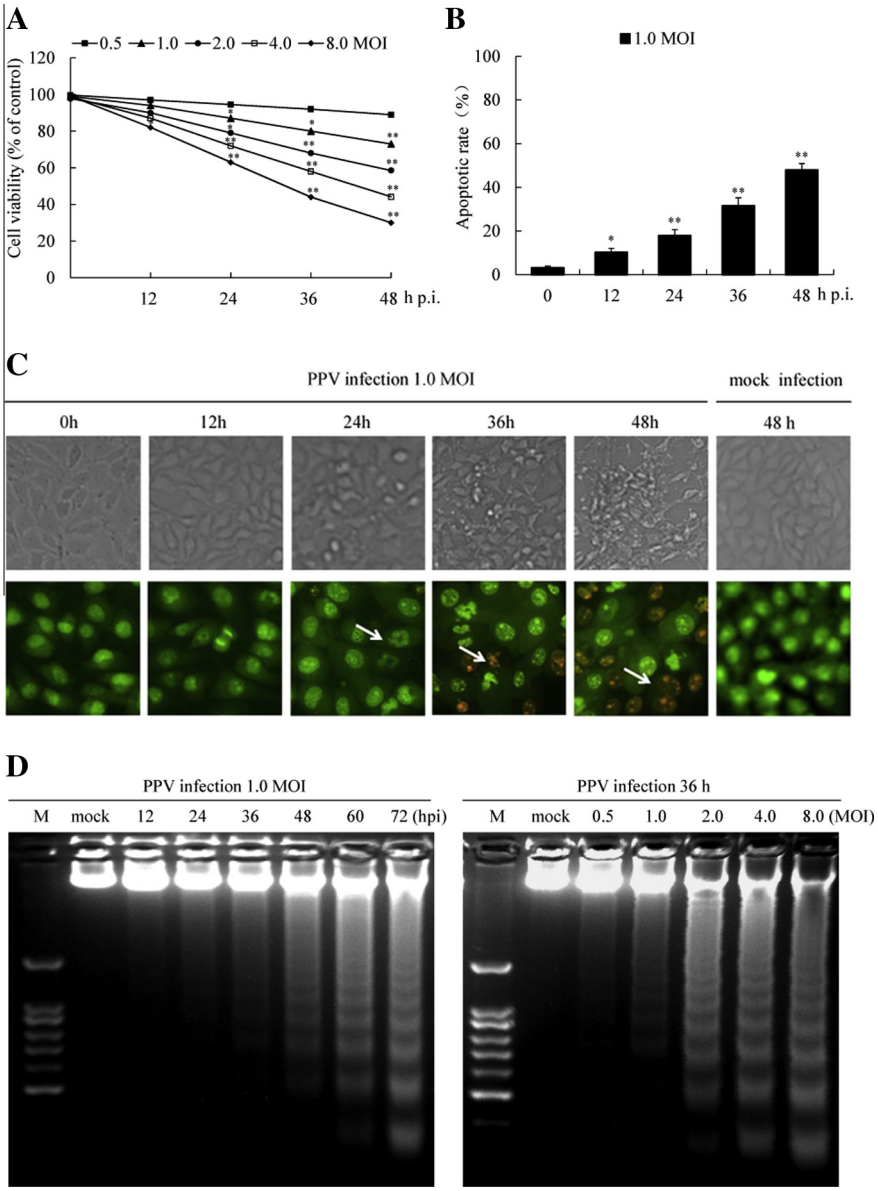

Fig. 1. PPV infection induced apoptosis in PK-15 cells. (A) The effect of PPV on cell viability. PK-15 cells were infected with PPV at different MOIs for the indicated times. Cell viability was measured by MTT assay. (B) Apoptosis rate of PPV-infected PK-15 cells. Cells infected with 1.0 MOI of PPV were stained with Annexin V-FITC and PI at indicated times and analyzed by flow cytometry. The Annexin V positive cells were regarded as apoptotic. (C) Morphological changes in PPV-infected cells. PK-15 cells were infected with PPV at 1.0 MOI for different times, mock infection at 48 h served as control. PPV-induced CPE was observed under inverted microscope (upper panel). Nuclear morphological changes were showed under fluorescence microscopy followed AO/EB staining (200 ×) (lower panel). Arrows showed condensed chromatin and nuclear fragmentation. (D) DNA fragmentation in PPV-infected cells. Cells were infected with PPV at 1.0 MOI for different times (left panel) or at different MOIs for 36 h (right panel), DNA was isolated and analyzed using agarose gel electrophoresis. Lane M, 100 bp DNA molecular weight marker. Lane mock (left panel), sham-infected for 72 h; lane mock (right panel), sham-infected for 36 h. The results are means ± SEM and representative of three independent experiments. $^{*}P < 0.05$, $^{**}P < 0.01$ versus the control group (0 h).

in PPV-infected cells. AO/EB staining showed that chromatin condensation and margination were visualized at 24 h p.i., nuclear fragmentation appeared at 36 h p.i., whereas there was no significant change appeared in mock infected cells (Fig. 1C, lower panel). Chromosomal DNA fragmentation assay showed that DNA ladder could be observed at 36 h p.i. in PK-15 cells infected with 1.0 MOI of PPV, and appeared to be more evident with time and dose of infection (Fig. 1D). These results suggested that PPV infection induced apoptosis in PK-15 cells.

3.3. PPV infection triggered apoptosis in PK-15 cells through induction of caspase activity

Activation of the caspase proteinases is a central event in the occurrence of apoptosis [19]. Therefore, we further measured the activity of several caspases which play pivotal roles in the activation of apoptotic pathway. As shown in Fig. 2A, when PK15 cells were infected with PPV at 1.0 MOI, the level of activated caspase-9 and -3 increased as early as 12 h p.i., but caspase-8 activity was not observed in this study. To determine the contribution of caspase-8 or -9 to activate caspase-3, we analyzed the inhibitory efficacy of caspase-8 or caspase-9 inhibitor in caspase-3 activity in PPV-infected cells. As shown in Fig. 2B, the activity of caspase-3 was significantly inhibited in caspase-9 inhibitor-treated cells, but was not in caspase-8 inhibitor-treated cells.

Caspase-3, as an effector caspase, can cleave some protein substrates to trigger the apoptotic process [20]. Therefore, we further determined the cleavage of PARP by western blot. As shown in Fig. 2C, the cleavage of PARP was detected after 12 h p.i., whereas

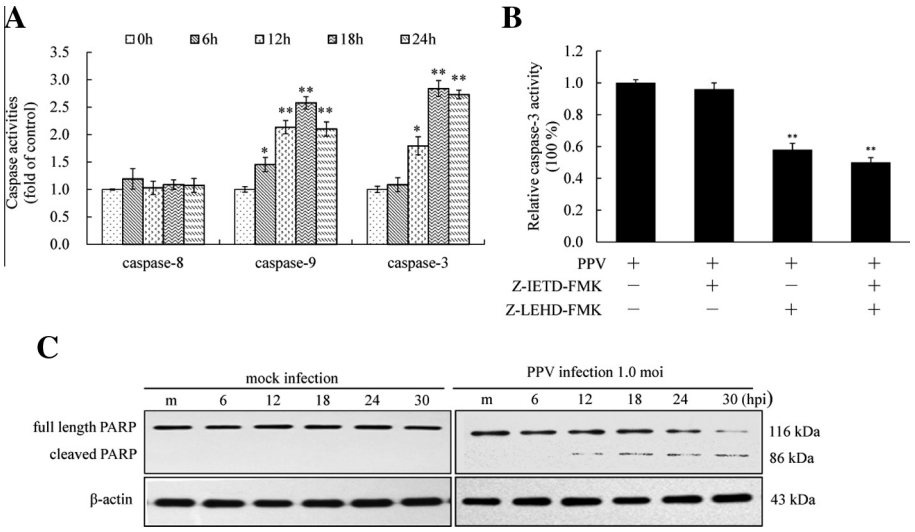

Fig. 2. The enzymatic activities of caspase-8, -9 and -3 in PPV-infected cells. (A) Caspase activity in PPV-infected cells. The activity of caspases-8, -9 and -3 in PK-15 cells infected with 1.0 MOI of PPV for indicated times were measured using the colorimetric assay kits. $^{*}P < 0.05$, $^{**}P < 0.01$ versus the control group (0 h). (B) The effect of initiator caspase-8 or -9 on the activation of caspase-3. Cells were incubated with 20 μM of caspase inhibitors for 1 h and then infected with 1.0 MOI of PPV for 24 h. Z-IETD-FMK and Z-LEHD-FMK were used to inhibit the activation of caspase-8 and caspase-9, respectively. $^{**}P < 0.01$ versus PPV infection alone without inhibitor for 24 h. (C) The cleavage of PARP in PPV-infected cells. PK-15 cells were infected with 1.0 MOI of PPV for indicated times. Expression level of PARP was analyzed by western blot. The values are means ± SEM and representative of three independent experiments.

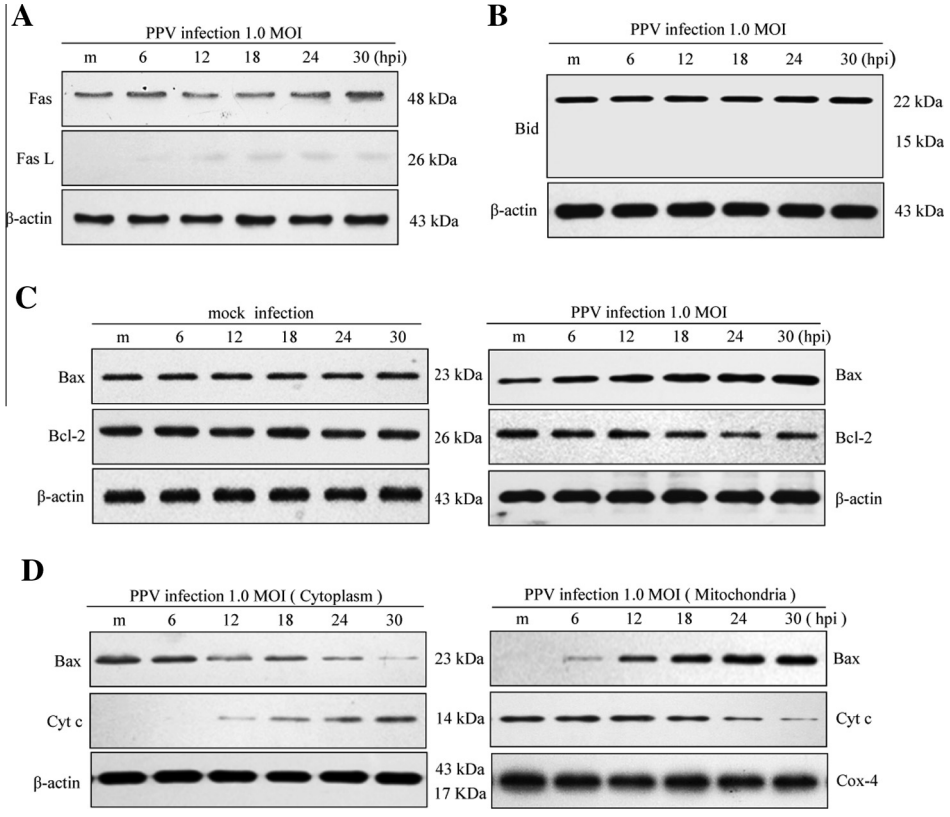

Fig. 3. PPV-induced apoptosis of PK-15 cells was mediated by the activation of mitochondrial pathway. PK-15 cells were infected with PPV at 1.0 MOI for indicated times. The cell lysates, cytosolic protein and mitochondrial protein were subjected to western blot analysis. (A) The expression of Fas or FasL in PPV-infected cells. (B) The cleavage of Bid in PPV-infected cells. (C) The changes of Bax and Bcl-2 in PPV-infected cells. (D) The translocation of Bax and release of mitochondrial cytochrome c (Cyt c) in PPV-infected cells. β-Actin and Cox-4 were used as endogenous controls for gene expression analysis of the cytosolic fractions and the mitochondrial fractions, respectively. All the data shown are representative of three independent experiments.

no cleaved PARP was detected in mock-infected cells. These results suggested that caspase-9 and -3 were activated in the PPV-induced apoptotic cells. Taken together, these results demonstrated that PPV infection triggered apoptosis in PK-15 cells through activation of caspase-9 and -3, but not caspase-8.

3.4. PPV induction of apoptosis was regulated by the mitochondria-mediated apoptotic pathway

Consistent with the nonactivated caspase-8, the expression of Fas and FasL did not appear significant changes in the process of

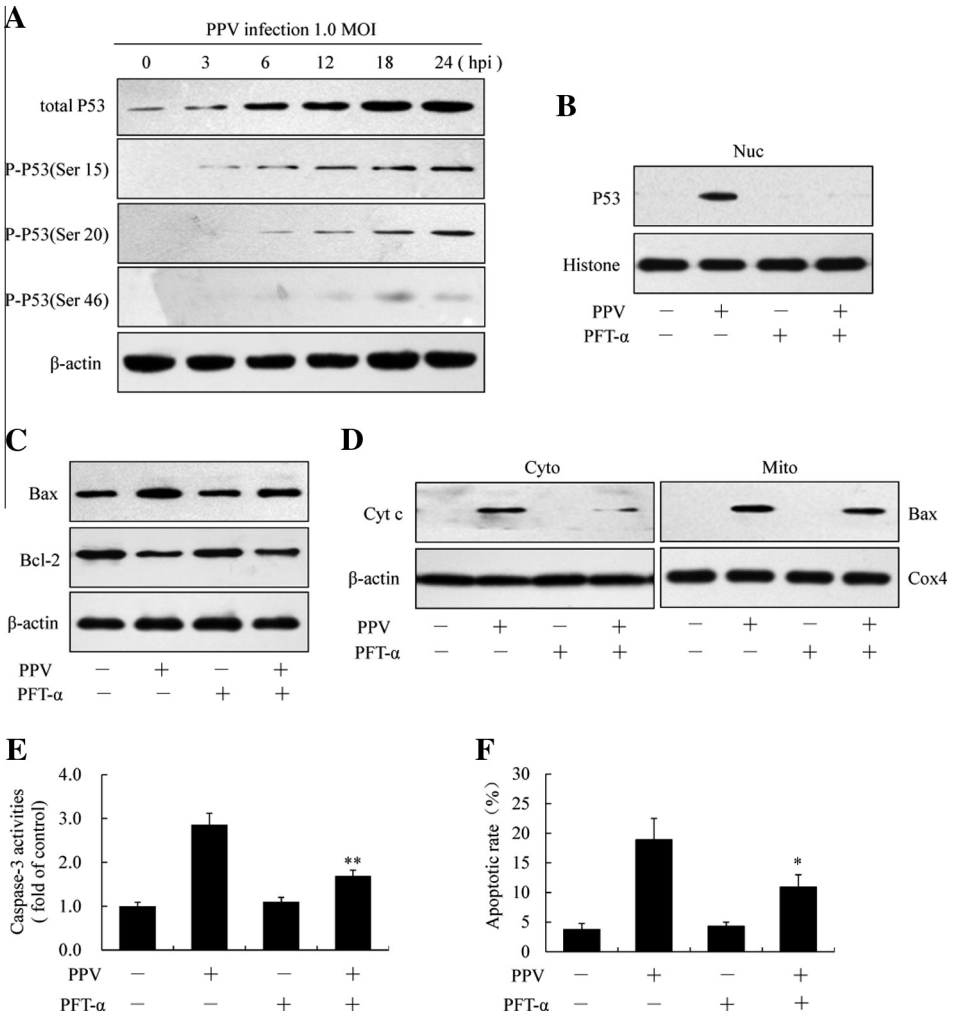

Fig. 4. The roles of p53 in PPV-induced cell apoptosis. PK-15 cells were pretreated with PFT-α (20 μM) for 1 h, and infected with PPV at 1.0 MOI for indicated times. (A) The accumulation and phosphorylation of p53 in PK-15 cells. Total protein was harvested for detection of p53 and p-p53 by western blot. (B) The effect of PFT-α on p53 translocation (from cytosol to nucleus) at 24 h p.i. Histone was measured as endogenous control for nuclear fractions. (C) The effects of PFT-α on the expression of Bax and Bcl-2 at 24 h p.i. (D) Effects of PFT-α on Bax translocation and cytochrome c (Cyt c) release at 24 h p.i. (E) Effect of PFT-α on activity of caspase-3 in PPV-infected cells. PFT-α treated cells were infected by PPV for 24 h, cell lysates were extracted for colorimetric assay. (F) Effect of PFT-α on apoptosis rate of PPV-infected cells at 24 h p.i. The values are means ± SEM of three independent experiments. $^{*}P < 0.05$, $^{**}P < 0.01$ versus PPV-infected cells without PFT-α treatment.

PPV-induced apoptosis (Fig. 3A), and cleavage of Bid was also hardly observed in PPV-infected cells by western blot (Fig. 3B), suggesting that the extrinsic pathway was not triggered in the process of PPV-induced apoptosis.

Next, we evaluated the expression of Bcl-2 family members and mitochondrial proteins in PK-15 cells infected with PPV at 1.0 MOI. Compared with mock infected cells, the level of pro-apoptotic Bax protein was gradually increased at 6 h p.i., while the expression of anti-apoptotic member Bcl-2 protein was decreased slightly in PPV-infected cells correspondingly (Fig. 3C), suggesting that PPV infection increased the ratio of Bax/Bcl-2, which was in favor of the disruption of mitochondrial function and the occurrence of apoptosis. Thus, we further analyzed the content of Bax and cytochrome c in the extract from either cytosol or mitochondria of PPV-infected cells. As shown in Fig. 3D, the level of Bax protein was found to be decreased in cytosol at 6 h p.i., accompanied by a corresponding increase in the mitochondrial fraction, while the release of mitochondrial cytochrome c (Cyt c) was observed at 12 h p.i., however, all of these changes could not be detected in mock infected cells. Taken together, these results suggested that the regulation of Bcl-2 family members and activation of mitochondria-mediated apoptotic pathway played pivotal roles in the apoptosis induced by PPV infection in PK15 cells.

3.5. Characterization of the p53 status in PPV induction of cell apoptosis

The mitochondrial pathway of apoptosis is tightly regulated by the transcription dependent mechanisms of p53 [21]. The protein stability and transactivation activity of p53 are associated with several posttranslational modifications, including N-terminus regions phosphorylation, nuclear localization and DNA binding activity [22]. To further investigate the upstream apoptotic signals in PPV-inducted apoptosis, we detected the levels and activity of p53. In PK-15 cells, PPV infection promoted the accumulation of total cellular p53 as early as 3 h p.i. compared to mock-infected controls and remained elevated till 24 h p.i. Phosphorylation of p53 at serine 15, 20 and 46 were detected at 3, 6, 12 h p.i., respectively (Fig. 4A). Pifithrin-α (PFT-α), a specific inhibitor of p53 signaling that inhibits p53-dependent transcription of p53-responsive genes, was used to detected the effects of p53 on PPV-induced mitochondria apoptotic pathway. Pretreatment of PK-15 cells with PFT-α blocked PPV-induced nucleus translocation of p53 (Fig. 4B), and interfered with the expression of Bax but no effect on Bcl-2 at 24 h p.i. (Fig. 4C). Then, the mitochondrial translocation of Bax and release of Cyt c were partially attenuated (Fig. 4D), followed by the distinct decrease of caspase-3 activity

in PFT-α treated cells (Fig. 4E). Compared to PPV-infected cells without PFT-α treatment, apoptosis rate of PFT-α treated cells was decreased from 18.89% to 10.93% ($P < 0.05$) (Fig. 4F). These results suggested that PPV infection promoted the accumulation and transcriptional activity of p53 to regulate the mitochondrion-mediated apoptosis pathway.

4. Discussion

Apoptosis is an important event in viral diseases pathogenesis and generally exhibits a series of morphological and molecular changes distinguished from other cell death subroutines [23]. In the present study, we observed that PPV infection induced evident apoptotic features in PK-15 cells, including chromatin condensation, DNA fragmentation and caspase-3/-9 activation, and found that p53, as a key regulator, modulated mitochondria-mediated apoptotic pathway to control the occurrence of apoptosis in PPV-infected PK-15 cells.

The activation of caspase cascades plays essential roles in initiation and execution of apoptosis induced by virus infection [24,25]. In PPV-infected cells, FasL was not detected. In addition, Bid, a specific proximal substrate of caspase-8, was not cleaved in PPV-infected cells, suggesting that Fas-mediated death receptor pathway was not involved in PPV induction of apoptosis. While the activation of caspase-9/-3 and cleavage of PARP indicated the potential of the mitochondria pathway. As predicted, PPV infection increased the expression of pro-apoptotic member Bax protein and decreased anti-apoptotic member Bcl-2, causing mitochondrial outer-membrane permeabilization, followed by release of cytochrome c and translocation of Bax, which contributed to the formation of apoptosome, then initiator caspase-9 and downstream executor caspases were activated. These results were consistent with the observation in canine [13] and murine [14] parvovirus, suggesting that apoptosis induced by PPV infection was mitochondrion-mediated.

Previous reports have provided that the p53 tumor suppressor protein is a transcriptional activator, regulating the expression of Bax, Bcl-2 and some other apoptotic genes [26,27]. Our studies demonstrated that PPV infection increased the accumulation and activity of p53 in PK-15 cells, which preceded caspases activity and expression changes of Bcl-2 family members. Phosphorylation of p53 at serine 15, 20 and 46 in PPV-infected cells enhanced the stability and transcriptional activity of p53, resulting in nuclear translocation of cytoplasmic p53 [28]. Specific inhibition of p53 translocation to nucleus by PFT-α decreased the expression and translocation of Bax. Suppression of Bax partially alleviated PPV-induced cytochrome c release and caspase-3 activation and might control the dysfunction of mitochondrial membrane potential [29]. These results indicated that p53 was required for induction of mitochondrion-mediated apoptosis pathway during PPV infection.

In conclusion, our results demonstrated that PPV infection impact on PK-15 cells fate through activation of p53 and mitochondria-mediated apoptosis signaling. Our results may shed light on the pathogenesis of PPV infection and provide insights into the relationship between host and PPV. However, the complete molecular mechanisms underlying PPV induction of cell death need to be unveiled deeply.

Author contributions

Hongling Zhang, Yong Huang and Dewen Tong conceived and designed the experiments; Hongling Zhang performed the experiments with assistance and advice from Qian Du, Xiaomao Luo, Liang Zhang, Xiaomin Zhao, Hongling Zhang and Yong Huang analyzed the data and wrote the paper; Yong Huang and Dewen Tong revised the manuscript. All authors have read the manuscript and approved for the submission.

Conflict of interest

The authors declare no conflict of interest.

Acknowledgments

This work was supported by the National Natural Science Foundation of China (Grant No. 31372401), Key Project of Shaanxi Province Science and Technology Innovation Team (2013KCT-28) and the Fundamental Research Funds for the Central Universities (ZD2013009 and Z111021103).

References

[1] A. Csagola, M. Lorincz, D. Cadar, K. Tombacz, I. Biksi, T. Tuboly, Detection, prevalence and analysis of emerging porcine parvovirus infections, Arch. Virol. 157 (2012) 1003–1010.
[2] R.C. Cutlip, W.L. Mengeling, Pathogenesis of in utero infection of eight- and ten weeks-old porcine fetuses with porcine parvovirus, Am. J. Vet. Res. 36 (1975) 1751–1754.
[3] T.W. Molito, H.S. Joo, Clinical and pathological features of porcine parvovirus related disease and its diagnosis, in: P. Tijssen (Ed.), CRC Handbook of Parvoviruses, CRC Press, Boca Raton, 1990, pp. 135–150.
[4] M. Narota, S. Inui, Y. Kawakami, K. Kitamura, A. Maeda, Histopathological changes of the brain in swine fetuses naturally infected with porcine parvovirus, Natl. Inst. Anim. Health Q. 15 (1975) 24–28.
[5] G.G. Hogg, C. Lenghaus, A.J. Forman, Experimental porcine parvovirus infection of foetal pigs resulting in abortion, histological lesions and antibody formation, J. Comp. Pathol. 87 (1977) 539–549.
[6] J.I. Kresse, W.D. Taylor, W.W. Stewart, K.A. Eernisse, Parvovirus infection in pigs with necrotic and vesicle-like lesions, Vet. Microbiol. 10 (1985) 525–531.
[7] K. Oraveerakul, C.S. Choi, T.W. Molitor, Tissue tropisms of porcine parvovirus in swine, Arch. Virol. 130 (1993) 377–389.
[8] K. Oraveerakul, C.S. Choi, T.W. Molitor, Reproductive failure in wild boars associated to porcine parvovirus infection and in vivo and in vitro characterization of the causal isolate, Trop. Anim. Health Prod. 42 (2010) 1611–161318.
[9] G.N. Barber, Host defense, viruses and apoptosis, Cell Death Differ. 8 (2011) 113–126.
[10] L. Ding, X.M. Zhao, Y. Huang, Q. Du, F. Dong, H.L. Zhang, D.W. Tong, Regulation of ROS in transmissible gastroenteritis virus-activated apoptotic signaling, Biochem. Biophys. Res. Commun. 442 (2013) 33–37.
[11] A.G. Granja, M.L. Nogal, C. Hurtado, J. Salas, M.L. Carrascosa, Y. Revilla, Modulation of p53 cellular function and cell death by African swine fever virus, J. Virol. 78 (2004) 7165–7174.
[12] S.M. Lee, S.B. Kleiboeker, Porcine reproductive and respiratory syndrome virus induces apoptosis through a mitochondria-mediated pathway, Virology 365 (2007) 419–434.
[13] J. Doley, L.V. Singh, G.R. Kumar, A.P. Sahoo, L. Saxena, U. Chaturvedi, S. Saxena, P.K. Singh, R.S. Rajmani, Canine parvovirus type 2a (CPV-2a)-induced apoptosis in MDCK involves both extrinsic and intrinsic pathways, Appl. Biochem. Biotechnol. 172 (2014) 497–508.
[14] A.Y. Chen, Y. Luo, F. Cheng, Y.N. Sun, J.M. Qiu, Bocavirus infection induces mitochondrion-mediated apoptosis and cell cycle arrest at G(2)/M phase, J. Virol. 84 (2010) 5615–5626.
[15] Y.C. Aaron, J.M. Qiu, Parvovirus infection-induced cell death and cell cycle arrest, Future Virol. 5 (2010) 731–743.
[16] L. Shi, Y. Huang, X.G. Xu, D.W. Tong, Sequence analysis of porcine parvovirus Y L Strain and Prokaryotic expression of *VP2*, Acta Agric. Bor.-Occi. Sin. 21 (2012) 6–12.
[17] L.J. Reed, H. Muench, A simple method of estimating fifty percent endpoints, Am. J. Epidemiol. 27 (1938) 493–497.
[18] L. Ding, X.G. Xu, Y. Huang, Z.C. Li, K. Zhang, G.D. Chen, G.S. Yu, Z.S. Wang, W. Li, D.W. Tong, Transmissible gastroenteritis virus infection induces apoptosis through FasL- and mitochondria-mediated pathways, Vet. Microbiol. 158 (2012) 12–22.
[19] A.K. Berger, P. Danthi, Reovirus activates a caspase-independent cell death pathway, Mbio 4 (2013), http://dx.doi.org/10.1128/mBio 00178-13.
[20] L. Marek, M. Malgorzata, F. Davide, S. Anna, S. Christopher, R. Andrea, H. Zdenko, Q.W. Zhao, S.O. Klaus, Activation and caspase-mediated inhibition of PARP: a molecular switch between fibroblast necrosis and apoptosis in death receptor signaling, Mol. Biol. Cell 13 (2002) 978–988.
[21] J.E. Chipuk, T. Kuwana, L. Bouchier-Hayes, N.M. Droin, D. Newmeyer, M. Schuler, D.R. Green, Direct activation of Bax by p53 mediates mitochondrial membrane permeabilization and apoptosis, Science 303 (2004) 1010–1014.
[22] K.H. Vousden, Activation of the p53 tumor suppressor protein, Biochim. Biophys. Acta 1602 (2002) 47–59.

[23] N. Yatim, M.L. Albert, Dying to replicate: the orchestration of the viral life cycle, cell death pathways, and immunity, Immunity 35 (2011) 478–490.
[24] T. El-Bacha, A.T. Da Poian, Virus-induced changes in mitochondrial bioenergetics as potential targets for therapy, Int. J. Biochem. Cell Biol. 45 (2013) 41–46.
[25] V.S. Marsden, L. O'Connor, L.A. O'Reilly, J. Silke, D. Metcalf, P.G. Ekert, D.C.S. Huang, F. Cecconi, K. Kuida, K.J. Tomaselli, Apoptosis initiated by Bcl-2-regulated caspase activation independently of the cytochrome c/Apaf-1/caspase-9 apoptosome, Nature 419 (2002) 634–637.
[26] X.D. Wang, X.F. Deng, W.J. Yan, Z.X. Zhu, Y. Shen, Y.F. Qiu, Z.X. Shi, D.H. Shao, J.C. Wei, X.Z. Xia, Stabilization of p53 in influenza A virus-infected cells is associated with compromised MDM2-mediated ubiquitination of p53, J. Biol. Chem. 287 (2012) 18366–18375.
[27] C.F. Silva, R. Gameiro, L.H. Okamura, E.F. Flores, T.C. Cardoso, Programmed cell death-associated gene transcripts in bovine embryos exposed to bovine Herpesvirus type 5, Mol. Cell. Probes 28 (2014) 113–117.
[28] S. Tadahis, J.T. Philip, S.S. Timothy, P. Dipen, T.J. Liu, F.L. Frederick, Apoptosis induced by adenovirus-mediated p53 gene transfer in human glioma correlates with site-specific phosphorylation, Cancer Res. 62 (2002) 1069–1076.
[29] T. Elizabeth, L. Kimberly, J. Jerem, T. Terrence, K. Kouacou, S.C. Stacey, Influenza virus infection increases p53 activity: role of p53 in cell death and viral replication, J. Virol. 79 (2005) 8802–8811.